

## LYMPHOID NEOPLASIA

# Fine-tuning of FOXO3A in cHL as a survival mechanism and a hallmark of abortive plasma cell differentiation

Clarissa D. Osswald,<sup>1</sup> Linka Xie,<sup>2</sup> Hanfeng Guan,<sup>3</sup> Franziska Herrmann,<sup>1</sup> Sarah M. Pick,<sup>1</sup> Marion J. Vogel,<sup>1</sup> Franziska Gehringer,<sup>1</sup> Fong Chun Chan,<sup>4</sup> Christian Steidl,<sup>4</sup> Thomas Wirth,<sup>1</sup> and Alexey Ushmorov<sup>1</sup>

<sup>1</sup>Institute of Physiological Chemistry, University of Ulm, Ulm, Germany; <sup>2</sup>Cancer Center of Union Hospital and <sup>3</sup>Department of Orthopaedic Surgery of Tongji Hospital, Tongji Medical College, HuaZhong University of Science and Technology, Wuhan, China; and <sup>4</sup>Department of Pathology and Laboratory Medicine, Centre for Lymphoid Cancers, Vancouver, BC, Canada

## KEY POINTS

- FOXO3A expression indicates an abortive PC differentiation state in cHL.
- Tight regulation of FOXO3A is essential for the cHL oncogenic program.

We recently found that FOXO1 repression contributes to the oncogenic program of classical Hodgkin lymphoma (cHL). Interestingly, FOXO3A, another member of the FOXO family, was reported to be expressed in the malignant Hodgkin and Reed-Sternberg cells of cHL at higher levels than in non-Hodgkin lymphoma subtypes. We thus aimed to investigate mechanisms responsible for the maintenance of FOXO3A as well as the potential role of FOXO3A in cHL. Here, we show that high FOXO3A levels in cHL reflect a B-cell-differentiation-specific pattern. In B cells, FOXO3A expression increases during the process of centroblast to plasma cell (PC) differentiation. FOXO3A levels in cHL were found higher than in germinal center B cells, but lower than in terminally differentiated PCs. This intermediate FOXO3A expression in cHL might manifest the "abortive PC differentiation" phenotype. This assumption was

further corroborated by the finding that overexpression of FOXO3A in cHL cell lines induced activation of the master PC transcription factor PRDM1 $\alpha$ . As factors attenuating FOXO3A expression in cHL, we identified *MIR155* and constitutive activation of extracellular signal-regulated kinase. Finally, we demonstrate the importance of FOXO3A expression in cHL using an RNA interference approach. We conclude that tightly regulated expression of FOXO3A contributes to the oncogenic program and to the specific phenotype of cHL. (*Blood*. 2018;131(14):1556-1567)

## Introduction

Classical Hodgkin lymphoma (cHL) derives from germinal or post-germinal center (GC) B cells.<sup>1</sup> In rare cases, a T-cell origin of cHL cells was reported.<sup>2</sup> cHL is characterized by a paucity of its malignant component, the Hodgkin and Reed-Sternberg (HRS) cells, which are outnumbered by immune cells of an inflammatory environment making up >98% of the tumor mass.<sup>3</sup> The oncogenic program of cHL includes activation of the NF- $\kappa$ B-, JAK-STAT-, and NOTCH-signaling pathways,<sup>4,5</sup> resulting in constitutive expression of MYC, IRF4, BCL2, and BCL2L1/BCL-xL proto-oncogenes, which are responsible for uncontrolled proliferation and resistance to apoptosis.<sup>1</sup> cHL differs from other B-cell non-Hodgkin lymphoma (NHL) entities by having almost completely extinguished their B-cell program. This includes the absence (POU2F2/OCT2, POU2AF1/BOB1) or inactivation (TCF3/E2A<sup>6,7</sup>) of B-cell-specific transcription factors and repression of their targets such as immunoglobulins, CD19, CD20, and CD79A.<sup>8,9</sup> At the same time, cHL harbors characteristics of abortive plasma cell (PC) differentiation. The abortive PC differentiation phenotype is associated with expression of both GC (BCL6<sup>10</sup> and PAX5<sup>11</sup>) and PC markers, including IRF4,<sup>12</sup> its direct target PRDM1 (although at low levels),<sup>13</sup> and CD138/syndecan-1.<sup>10</sup> A comparative epigenetic profiling of cHL and myeloma cell lines also supported the hypothesis of an abortive PC phenotype

in cHL.<sup>14</sup> Interestingly, presence of PC characteristics like activation of NF- $\kappa$ B and JAK-STAT signaling, and expression of IRF4 in cHL, does not result in substantial PRDM1 production and immunoglobulin secretion.<sup>4,13,14</sup> The partial block of PRDM1 expression might contribute to cHL lymphomagenesis as PRDM1 has been shown to act as a tumor suppressor both in cHL<sup>15</sup> and in activated B-cell diffuse large B-cell lymphoma, which has an oncogenic program similar to cHL.<sup>16-18</sup> Recently, we identified the transcription factor FOXO1 as tumor suppressor in cHL<sup>19</sup> and found that FOXO1 repression contributes to downregulation of PRDM1 $\alpha$ , an active isoform of PRDM1.<sup>15</sup>

FOXO1 belongs to the FOX O family of forkhead transcription factors, which share high homology in the DNA-binding forkhead domain.<sup>20</sup> FOXO family transcription factors have been intensively studied due to their versatile effects on critical cellular processes including differentiation, cell death, proliferation, and protection against reactive oxidative species.<sup>21</sup> The FOXO family comprises 4 members: FOXO1, FOXO3, FOXO4, and FOXO6. Their role in PC differentiation is not clear. Knockout of *Foxo1* or *Foxo3a* does not repress PC generation in mouse models.<sup>22,23</sup> In contrast, knockout of 14-3-3 $\sigma$ /stratifin, the protein responsible for nuclear export of FOXOs, leads to faster proliferation and differentiation of mouse B cells into immunoglobulin G<sub>3</sub>-positive

plasmablasts.<sup>24</sup> Moreover, *FOXO3* is strongly induced in human B cells committed to PC differentiation in vitro.<sup>25,26</sup>

Interestingly, *FOXO3A* was detected in HRS cells but only in limited numbers of NHLs.<sup>27,28</sup> We thus hypothesized that the maintenance of *FOXO3A* contributes to the oncogenic program of cHL. *FOXO3A* expression might not only reflect the aborted PC differentiation process and the specific phenotype of cHL, but also facilitate its oncogenic transformation.

We found that cHL shares a unique pattern of *FOXO3A*/*FOXO1* expression with PCs and that *FOXO3A* levels are tightly regulated in cHL.

## Material and methods

### Cell lines and treatment

All cell lines were cultured at standard conditions and the authenticity of the cell lines was confirmed by short-tandem-repeat DNA typing as described in supplemental Methods (available on the *Blood* Web site). Clones of KM-H2 and L428 stably expressing *FOXO3(A3)ER* were generated by transfection of the cell lines with pcDNA-*FOXO3(A3)ER* vectors followed by selection with 1 mg/mL G418 sulfate (Calbiochem, Darmstadt, Germany). Nuclear translocation of *FOXO3(A3)ER* was induced by adding 4-hydroxytamoxifen (4-OHT; Calbiochem) at a final concentration of 200 nM.

Tonsillar CD19<sup>+</sup> cells were isolated by positive selection using microbeads (Miltenyi Biotec) as described previously.<sup>29</sup>

### Vectors and transduction

The phosphorylation-insensitive pcDNA-*FOXO3(A3)ER* vector was cloned from pBABE-*FOXO3(A3)ER*<sup>30</sup> (donated by P. J. Coffer, Utrecht, The Netherlands) into the pcDNA3.1(+) vector. We performed luciferase reporter assays to measure the functional activity of the *FOXO* expression vectors. The construct expressing *FOXO3A* tagged by a biotin ligase recognition signal (b*FOXO3*) was generated in a similar way as described for *FOXO1*.<sup>15</sup> The open reading frame of a constitutively active myristoylated version of AKT<sup>31</sup> (myrAKT; Addgene) was cloned into the SF-LV-cDNA-EGFP vector as described in supplemental Methods. *FOXO1* and *FOXO3A* short hairpin RNAs (shRNAs) as well as scrambled control were overexpressed with the help of the lentiviral pRS112-U6-sh-UbiC-TagRFP-2A-puro vector (Cellecra [https://www.cellecra.com/]) obtained from BioCat (Heidelberg, Germany). Lentiviral particles were produced as described in supplemental Methods.

### ChIP

Chromatin immunoprecipitation (ChIP) was done as described earlier for *FOXO1*<sup>15</sup> with the exception that the b*FOXO3*-pCDNA3.1 vector was used. A short protocol is given in supplemental Methods.

### Luciferase reporter assay

The luciferase reporter assay was done as described<sup>15</sup> (for details, see supplemental Methods).

### RT-qPCR and immunoblotting

RNA was isolated, complementary DNA (cDNA) generated, quantitative reverse transcription polymerase chain reaction

(RT-qPCR) was performed and data were analyzed by the  $\Delta\Delta$  cycle threshold method as we described<sup>15</sup> (for the list of primers, see supplemental Methods).

Immunoblot was done as we described.<sup>15</sup> A detailed description and the list of antibodies are available in supplemental Methods.

### Analysis of *FOXO* expression data using GENEVESTIGATOR

To compare *FOXO1* and *FOXO3A* expression levels at normal stages of B-cell differentiation (root: anatomy) and cHL (root: cancer), data were mined from public repositories by the web-based GENEVESTIGATOR software (https://genevestigator.com/; 04.14.2017).<sup>32</sup> The following probe sets were used in our studies: *FOXO1*, probe set 202724\_s\_at; *FOXO3A*, probe set 204131\_s\_at; *FOXO4*, probe set 205451\_at; *FOXO6*, probe set 239657\_x\_at. GENEVESTIGATOR uses probe sets that are validated by RT-qPCR across several organisms.<sup>33</sup> The 202724\_s\_at probe set targeting *FOXO1* was already used in our previous publication due to its high Jetset score<sup>34</sup> and was verified by RT-qPCR and immunoblot analysis.<sup>35</sup> The probe set 204131\_s\_at for *FOXO3A* also shows high correlation with RT-qPCR data.<sup>36</sup>

### Correlation analysis

To investigate the correlation between *PRDM1* and *FOXO3* messenger RNA (mRNA) levels in 29 microdissected HRS cells, data were mined from the Gene Expression Omnibus (GEO) data repository (http://www.ncbi.nlm.nih.gov/geo/; GSE39133). Probe set 228964\_at was used for *PRDM1* and probe set 224891\_at for *FOXO3* analysis. The probe set for *PRDM1* was already confirmed in our previous study<sup>15</sup> and the expression of the *FOXO3* probe set is known to be increased in PCs.<sup>37</sup> The probe set 224891\_at for *FOXO3* also shows higher specificity for *FOXO3A* than for its pseudogene *FOXO3B* (www.genecards.org; 01.15.2018).

### MIR155 measurement and inhibition

To inhibit *MIR155*, we used a specific miScript microRNA (miRNA) inhibitor (anti-hsa-miR-155-5p; Qiagen). L428 cells were transfected by nucleofection (Lonza) with 2  $\mu$ M of the specific miRNA inhibitor or with the miScript miRNA-negative control RNA. Cells were harvested for miRNA 24 hours, and for protein isolation 72 hours after transfection. miRNA was isolated using the Pure-Link miRNA Isolation kit (Invitrogen), and cDNA was synthesized with the miScript Reverse Transcription kit (Qiagen). *MIR155* expression was detected by RT-qPCR using the Hs\_miR-155\_2 miScript Primer Assay (Qiagen) and the miScript SYBR Green PCR kit (Qiagen). U6 served as reference gene. Primer sequences for U6 were forward 5'-CTCGCTTCGGCAGCAC and reverse 5'-AACGCTT CACGAATTTGCGT.

### Viability and cell-death analysis

Viability of cells was assessed using the trypan blue exclusion method on days 0, 2, 4, and 6 after activation of *FOXO3A*. Cells were counted with a hemacytometer. Cell death was assessed by Annexin V-fluorescein isothiocyanate/propidium iodide (PI) and by recording the stained cells with a FACSCanto II cytometer (BD Biosciences). Specific cell death was calculated

using the following formula: specific cell death (%) =  $100 \times (D_{ex} - D_c)/(100 - D_c)$ .  $D_{ex}$  equals the percentage of dead cells in the treated sample and  $D_c$  of the control sample. Dead cells were defined as either single or double positive for Annexin V and/or PI (see supplemental Methods for further details).

### Cell-cycle analysis

A total of  $1 \times 10^6$  cells were washed with phosphate-buffered saline, fixed in ice-cold 70% ethanol, and incubated on ice for at least 1 hour. After centrifugation and resuspension in phosphate-buffered saline containing 40  $\mu\text{g}/\text{mL}$  PI (Sigma-Aldrich) and 100  $\mu\text{g}/\text{mL}$  RNaseA (Amersham), cells incubated for 1 hour at room temperature. Cell cycle was measured by flow cytometry using a FACSCalibur flow cytometer (BD Biosciences) and the percentage of cells in the different cell-cycle phases was analyzed with help of ModFit LT version 2.0 software (Verify Software House, Topsham, ME).

## Results

### FOXO3A is highly expressed in cHL

To clarify the role of FOXOs in the process of PC differentiation and in the oncogenic program of cHL, we first used the GENEVESTIGATOR tool to compare the expression of FOXO transcription factors at different stages of B-cell differentiation to microdissected HRS cells of cHL. As we and others showed earlier,<sup>19,38,39</sup> centroblasts (CBs) expressed the highest levels of FOXO1. We observed that FOXO1 then gradually decreased during the process of terminal B-cell maturation into PCs. In contrast, FOXO3A levels progressively increased. With regard to cHL, we found that FOXO1 expression in HRS cells was similar to that of PCs. Remarkably, FOXO3A expression in HRS cells was lower than in PCs, but significantly higher than in GC B cells (Figure 1A). FOXO4 and FOXO6 were expressed at much lower levels than FOXO3A at all stages of mature B-cell differentiation, and their expression levels in cHL were even below that of FOXO1 (Figure 1A).

Next, we validated the GEP results by analyzing FOXO1 and FOXO3A expression in normal CD19<sup>+</sup> B cells and in B-cell-derived (KM-H2,<sup>40,41</sup> L428,<sup>41,42</sup> U-HO1,<sup>43</sup> L1236,<sup>44</sup> and SUP-HD1<sup>41,45</sup>) and T-cell-derived (HDLM2<sup>41</sup> and L540<sup>41,46</sup>) cHL cell lines using RT-qPCR and immunoblot (Figure 1B-H). In accordance with previous data,<sup>19</sup> FOXO1 mRNA expression in all cHL cell lines was lower than in CD19<sup>+</sup> B cells (Figure 1B). Of note, expression of FOXO1 in HDLM2, a T-cell-derived cHL cell line, was higher than in B-cell-derived cells. On the contrary, expression of FOXO3A in B-cell cHL cell lines was higher than in normal B cells and, in most cases, higher than in T-cell-derived cHL cell lines (Figure 1C). To identify the predominant FOXO family member in cHL cell lines and to point out possible differences between B- and T-cHL with regard to their FOXO expression levels, we also calculated FOXO3A/FOXO1 mRNA ratios. We found that FOXO3A is the main FOXO subtype in B-cell cHL, whereas T-cell-derived cHL cell lines showed an inverse FOXO mRNA expression profile (Figure 1D). A high FOXO3A-to-FOXO1 ratio in B-cell-derived cHL cell lines was also seen at the protein level, except for SUP-HD1 (Figure 1E-H).

Thus, cHL expresses FOXO3A levels intermediate between GC B cells and PCs, which further indicates the abortive PC phenotype of cHL. In addition, B- and T-cHL maintain different FOXO3A/FOXO1 expression patterns, which may reflect their different origin.

### FOXO3A directly induces PRDM1 $\alpha$ expression in cHL cell lines

Recently, we found that FOXO1 induces PRDM1 $\alpha$  in cHL cell lines, suggesting that repression of FOXO1 might contribute to the arrest of PC differentiation in cHL.<sup>15</sup> Considering our new finding, we asked whether the maintenance of FOXO3A expression might explain the intermediate levels of PRDM1 in cHL.

We first reanalyzed our GEP data of microdissected HRS cells<sup>4</sup> and found a positive correlation between FOXO3 and PRDM1 mRNA expression (Figure 2A). We were aware that both PRDM1 and FOXO3A are located on Chr 6q21, a region that is frequently deleted in B-cell NHL<sup>47</sup> and in cHL.<sup>4</sup> In fact, we identified a significant positive correlation between PRDM1 and FOXO3A copy-number states (supplemental Figure 1). Yet, there was no significant correlation between PRDM1 expression and its corresponding copy number in HRS cells, thus indicating the role of transcriptional regulation for PRDM1 expression.<sup>15</sup> To see whether there is a direct effect of FOXO3A on PRDM1 transcription, we generated KM-H2 and L428 cell lines stably expressing an inducible constitutively active variant of FOXO3A (FOXO3(A3)ER). Expression of the transgene and its functional activity in cHL cell lines was proven by immunoblot and luciferase reporter assay, respectively (Figure 2B-C). Activation of FOXO3A by 4-OHT strongly induced expression of PRDM1 $\alpha$  at mRNA and protein levels in both cell lines (Figure 2D-E, respectively). Expression of PRDM1 $\beta$ , a truncated variant of PRDM1 with strongly reduced repression activity, was not increased by FOXO3A (Figure 2E). We then analyzed the effect of FOXO3A on the transcriptional activity of PRDM1 $\alpha$  and PRDM1 $\beta$  promoters using a luciferase reporter assay. FOXO3A activated only the PRDM1 $\alpha$  but not the PRDM1 $\beta$  promoter (Figure 2F).

We have previously shown that FOXO1 can bind to FOXO-binding sites on the PRDM1 $\alpha$  promoter region by ChIP.<sup>15</sup> To demonstrate direct binding of FOXO3A to the PRDM1 $\alpha$  promoter, we generated a construct expressing the constitutively active form of FOXO3A tagged by a biotin ligase recognition signal (bFOXO3). Efficient biotinylation by the humanized version of the bacterial biotin ligase BirA and preservation of antigenic specificity was confirmed by pulling down bFOXO3 with streptavidin magnetic beads followed by immunoblot analysis (supplemental Figure 2A). The integrity of the transactivation activity of the tagged construct was confirmed by a luciferase reporter assay (supplemental Figure 2B). We tested binding of bFOXO3 to the promoter regions at positions -549, -832, and -953 upstream of the PRDM1 $\alpha$  transcription start site. As controls, we used the gene desert locus on chromosome 12 (Chr12) containing no FOXO1-binding sites and the FOXP1 enhancer region where FOXO3A is known to bind directly.<sup>48</sup> Quantification of the precipitated chromatin showed enrichment of all 3 PRDM1 $\alpha$  promoter regions. No binding was detected at the gene desert locus whereas strong interaction at the FOXP1

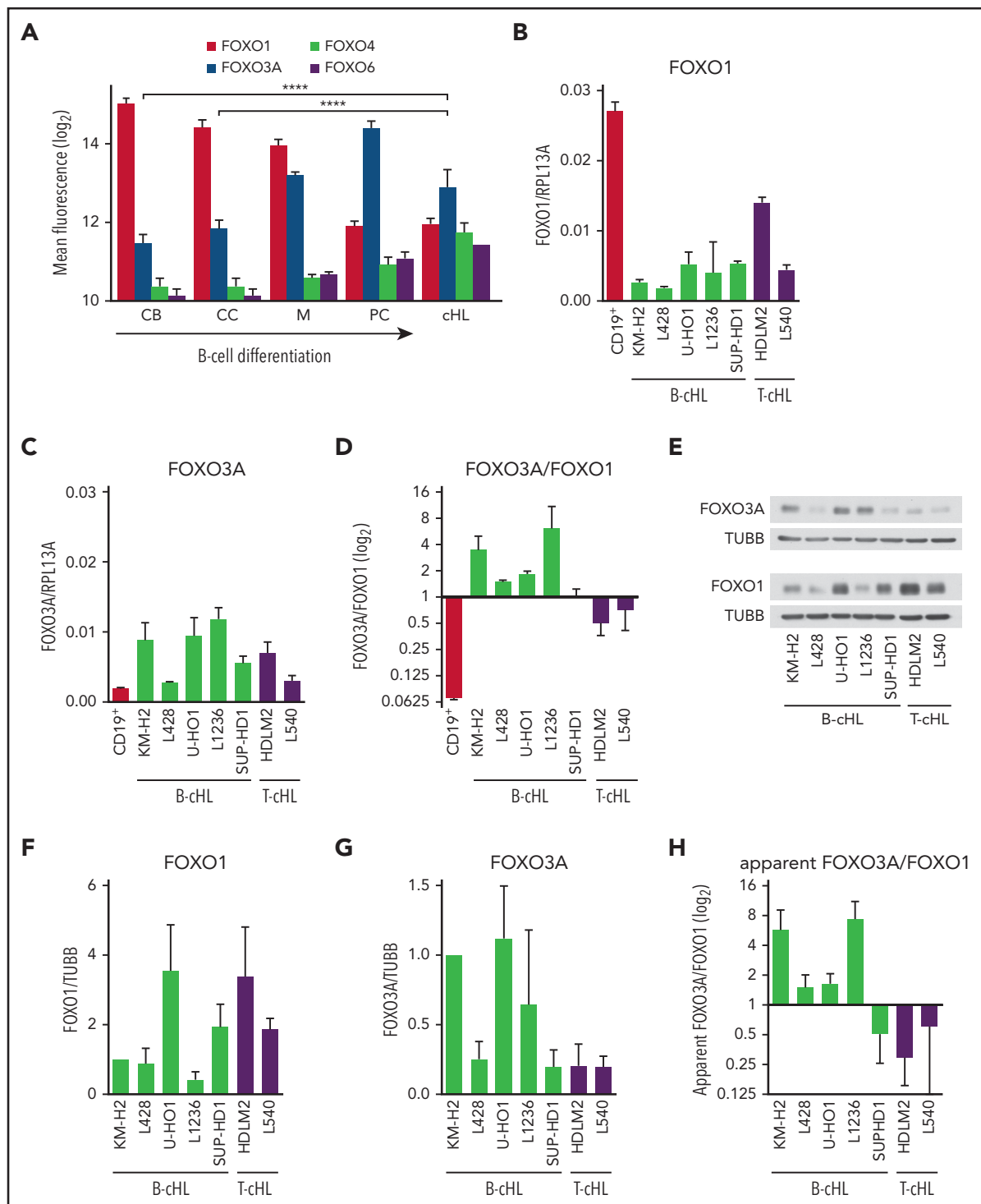


**Figure 1. FOXO3A is highly expressed in cHL.** (A) Gene expression profiling (GEP) data were mined and analyzed with help of the GENEVESTIGATOR software. The following data sets were used for analysis: CB and CC (GSE15271, GSE38697, GSE56314); M (GSE1266, GSE45113, GSE17186, GSE64028); PC (GSE12366, GSE45537, GSE56464, GSE5900), cHL (GSE14879). FOXO1: probe set 202724\_s\_at; FOXO3A: probe set 204131\_s\_at; FOXO4: probe set 205451\_at; FOXO6: probe set 239657\_x\_at. CB (n = 15); centrocytes (CC; n = 15); memory B cells (M; n = 38); PC (n = 13); microdissected HRS cells of cHL (cHL; n = 4). Data are represented as mean fluorescence  $\pm$  standard deviation (SD). Means of FOXO3A levels in GC B cells and cHL were compared using an online software ([https://www.medcalc.org/calc/comparison\\_of\\_means.php](https://www.medcalc.org/calc/comparison_of_means.php); 10.23.2017). \*\*\*\* $P < .0001$ . (B-H) FOXO1 and FOXO3A mRNA and protein expression in CD19<sup>+</sup> B cells and B- or T-cell-derived cHL cell lines. FOXO1 (B) and FOXO3A (C) mRNA levels were measured by RT-qPCR and expressed as ratio to RPL13A. Data are shown as mean  $\pm$  SD of 3 independent experiments. FOXO1 and FOXO3A expressions of all cHL cell lines except for FOXO3A in L540 significantly differed from CD19<sup>+</sup> B cells with  $P < .01$ . Statistical significances were analyzed by 2-tailed t tests. (D) FOXO3A/FOXO1 mRNA ratio in B cells and cHL. Data were extracted from experiments shown in panels B and C. (E) FOXO1 and FOXO3A protein expression was measured by immunoblot. The most representative of 3 independent analyses is shown. TUBB served as loading control. (F-G) The immunoblots were quantified using ImageJ 64 software. FOXO1 (F) and FOXO3A (G) values were normalized to TUBB. Data are shown as mean  $\pm$  SD of 3 independent experiments and values for KM-H2 were set to 1. (H) The apparent FOXO3A-to-FOXO1 ratio for each sample was calculated as: (FOXO3A/TUBB)/(FOXO1/TUBB). The apparent ratio does not represent the molar FOXO3A-to-FOXO1 ratio but permits to compare relative expression of FOXO proteins in different samples.

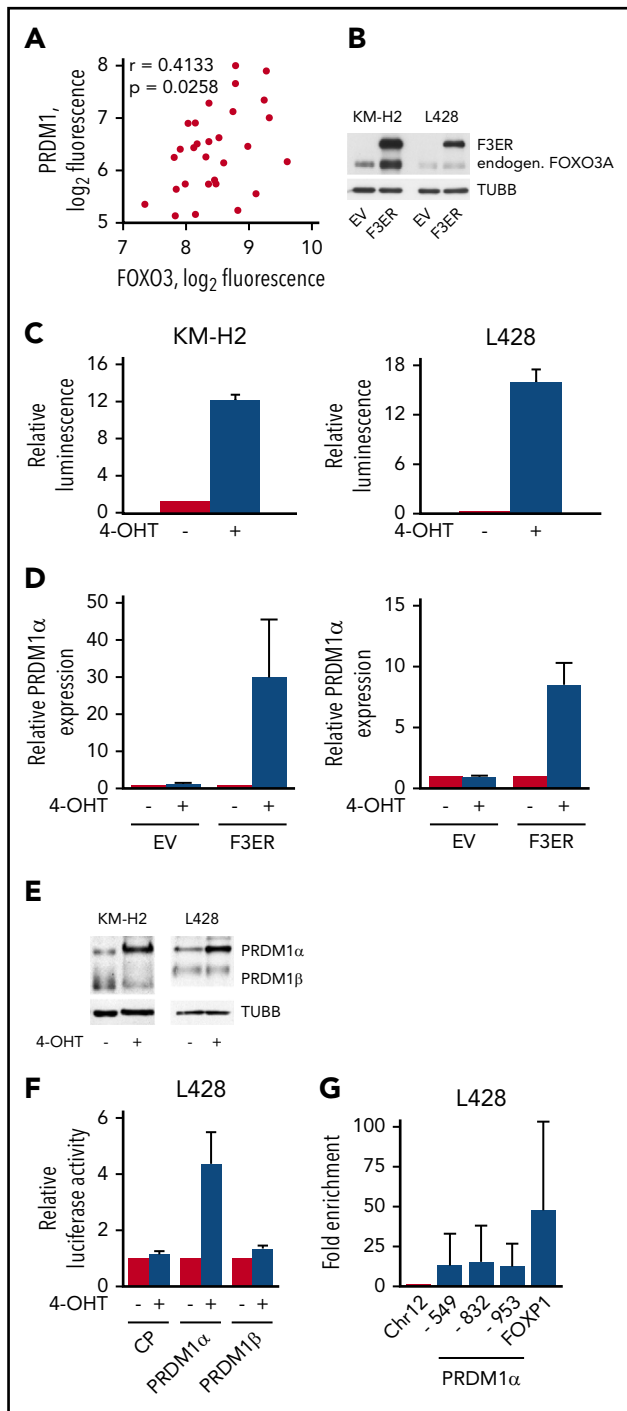


**Figure 2. FOXO3A directly activates PRDM1 $\alpha$  in cHL cell lines.** (A) PRDM1 and FOXO3 mRNA levels positively correlate in microdissected HRS cells. Data were mined from GEO (GSE39133). PRDM1, probe set 228964\_at; FOXO3, probe set 224891\_at. Statistical significance was analyzed by a 2-tailed Student *t* test. *r*, Pearson correlation coefficient. (B-F) The cHL cell lines KM-H2 and L428 expressing the constitutively active version of human FOXO3A (FOXO3(A3)ER [F3ER]) or EV were treated with 200 nM 4-OHT for 24 hours to induce nuclear translocation of the construct. (B) F3ER protein expression in stable cHL cell lines was assessed by immunoblot analysis. (C) Functional activity of F3ER in stably transfected cHL cell lines was demonstrated by transfection with a reporter vector containing the forkhead response element upstream of firefly luciferase and cotransfection with a *Renilla* luciferase reporter under the control of the ubiquitin promoter. F3ER was activated by 4-OHT immediately after transfection. Luminescence was measured as described in "Materials and methods." Bars indicate average firefly luciferase activity normalized to *Renilla* luciferase luminescence. (D-E) FOXO3A increases PRDM1 $\alpha$  mRNA (D) and protein (E) expression levels. cHL cells

enhancer was seen (Figure 2G). Thus, FOXO3A directly activates PRDM1 $\alpha$  transcription in cHL.

### FOXO3A activation results in growth arrest and induces negative regulators of the cell cycle in cHL cell lines

To analyze whether ectopic overexpression of FOXO3A affects proliferation and/or survival of cHL cell lines, we used KM-H2 and L428 cells stably expressing FOXO3(A3)ER. Compared with the empty vector (EV) control, activation of FOXO3A by 4-OHT significantly reduced the number of viable cells in both cHL cell lines (Figure 3A). The decrease of cell numbers was accompanied by significant, but minor, cell death (Figure 3B). In contrast, we found that FOXO3A strongly diminished the proportion of cells in the S phase and induced accumulation of cells in the G<sub>0</sub>/G<sub>1</sub> phase (Figure 3C). To clarify the molecular mechanisms of FOXO3A-induced cell-cycle arrest, we measured the expression of the FOXO-dependent cell-cycle inhibitors CDKN1A/p21 and CDKN1B/p27 as well as expression of CCND2 and MYC. Given that FOXOs inhibit the expression of cyclins and MYC by induction of BCL6, we also measured expression of these genes.<sup>49,50</sup> As expected, FOXO3A repressed CCND2 and upregulated CDKN1A and CDKN1B at the mRNA level in both cell lines (Figure 4A). MYC was more strongly repressed on protein than on mRNA level (Figure 4B-C), which can be explained by a decrease in MYC protein stability<sup>51</sup> or induction of MYC-targeting miRNAs.<sup>52</sup> In contrast, BCL6 mRNA levels were significantly increased after FOXO3A activation (Figure 4D). This was also confirmed on the protein level (Figure 4E).

We conclude that overexpression of FOXO3A in cHL has tumor-suppressor activity and that this is associated with repression of important inducers of cell proliferation like CCND2 and MYC, activation of the cell-cycle inhibitors CDKN1A and CDKN1B, as well as with upregulation of PRDM1 $\alpha$ .

### MIR155 and extracellular signal-regulated kinase contribute to FOXO3A attenuation in cHL

Recently, we have shown that multiple mechanisms including genomic deletions and miRNAs are involved in FOXO1 repression in cHL.<sup>19</sup> Given that FOXO3A deletions are frequent and correlate with a decrease of FOXO3A expression in HRS,<sup>4</sup> and that FOXO3A activation negatively regulates proliferation

**Figure 2 (continued)** expressing F3ER were treated with 200 nM 4-OHT or vehicle. mRNA and protein was isolated and analyzed via RT-qPCR or immunoblot, respectively. (F) FOXO3A activates the PRDM1 $\alpha$  promoter. L428 cells expressing F3ER were transiently transfected with the pGL4.20 vector containing the FOXO1 core promoter (CP) or a vector containing PRDM1 promoter regions, together with ubi-*Renilla* as reference vector. The FOXO1 CP, which does not contain FOXO-binding sites, served as negative control. After transfection, cells were treated with 4-OHT or vehicle and relative luciferase activity was measured 24 hours later. (G) FOXO3A directly binds to the PRDM1 $\alpha$  promoter. L428 cells were transfected with bFOXO3 and BirA or with EV and BirA. Twenty-four hours later, cells were harvested and ChIP was performed. The position of targeted FOXO-binding sites at PRDM1 $\alpha$  promoter regions is indicated counting from the start of transcription. A FOXO1 enhancer region served as positive control. The precipitated chromatin was amplified by specific primers and quantified with qPCR. Data are shown as fold enrichment compared with the gene desert region located on Chr12. All data are shown as mean  $\pm$  SD of 3 independent experiments. For immunoblots, a representative of 3 independent experiments is depicted. TUBB served as loading control.



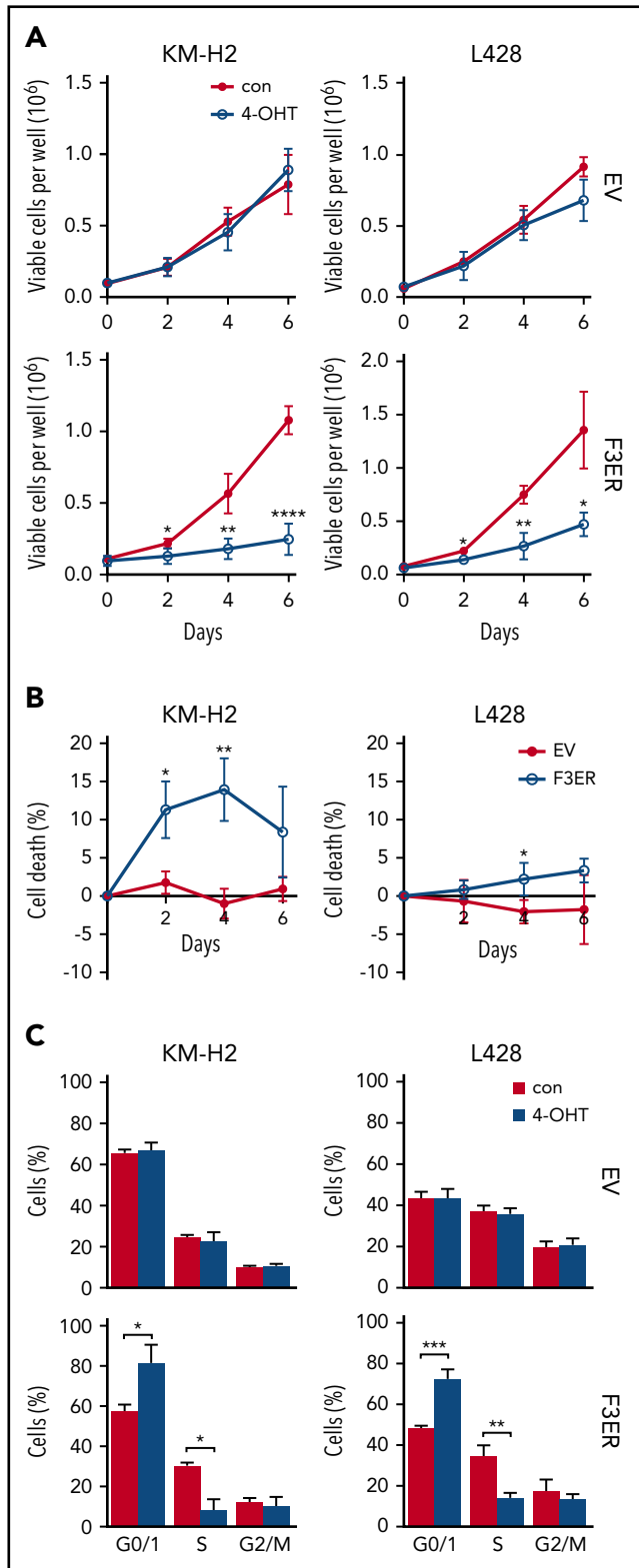


**Figure 3. FOXO3A induces growth arrest.** (A) FOXO3A inhibits growth of cHL cell lines. Cells transfected with a vector containing FOXO3(A3)ER (F3ER) or EV were seeded in 6-well plates at a density of  $0.05 \times 10^6$  cells per mL. Twenty-four hours later, cells were treated with 4-OHT or vehicle. Live cells were counted with a hemacytometer at indicated time points after seeding. Data represent mean  $\pm$  SD of 3 independent experiments. (B) F3ER- and EV-expressing cells were treated or not treated with 200 nM 4-OHT. Cell death was examined at indicated time points by staining with Annexin V/PI. Specific cell death was calculated as described in "Material and methods" and is shown as mean  $\pm$  SD of 3 independent experiments.

of cHL cells, we searched for additional mechanisms that regulate FOXO3A expression in cHL. The oncogenic *MIR155*, which is responsible for FOXO3A repression in glioma,<sup>53</sup> is known to be highly expressed in cHL.<sup>54</sup> Using a loss-of-function approach, we assessed the contribution of FOXO3A to attenuation of FOXO3A in cHL. Transient transfection of L428 with anti-*MIR155* efficiently decreased *MIR155* levels (Figure 5A), upregulated FOXO3A protein expression (Figure 5B-C), and increased the proportion of cells in the G<sub>0</sub>/G<sub>1</sub> phase (Figure 5D).

Given that constitutive extracellular signal-regulated kinase (ERK) activation in cHL contributes to FOXO1 downregulation,<sup>19</sup> we further studied the effect of ERK inactivation on FOXO3A expression. We observed that the ERK inhibitor U0126 dose-dependently increased FOXO3A protein levels in both KM-H2 and L428 (Figure 5E-F).

Taken together, high expression of *MIR155* and ERK activation controls FOXO3A levels in cHL.

### Maintenance of FOXO3A expression might contribute to survival and proliferation of cHL

Although FOXO3A expression is attenuated by genetic and epigenetic mechanisms, cHL expresses measurable amounts of FOXO3A indicating its contribution to the oncogenic program. We thus set out to investigate whether cHL cell lines are sensitive to expression of myrAKT, a constitutively active version of the FOXO-inactivating kinase AKT.<sup>31</sup> We found that myrAKT negatively regulated proliferation of KM-H2, L428, U-HO1, HDLM2, and L540 cell lines. At the same time, myrAKT expression did not influence the growth of L1236 and SUP-HD1 where AKT is known to be constitutively active (Figure 6A).<sup>19</sup> The effect of myrAKT on FOXO3A and FOXO1 expression and on their phosphorylation status was measured by immunoblot. myrAKT expression increased FOXO1/FOXO3A-inactivating phosphorylation in all cell lines except for SUP-HD1. In addition, myrAKT downregulated FOXO3A expression in KM-H2, L428, and L540, and FOXO1 in KM-H2, L428, L540, and SUP-HD1 (Figure 6B). Next, we used an RNA interference approach to specifically downregulate FOXO3A (2 different shRNAs) or FOXO1 (3 shRNAs) (Figure 6C and supplemental Figure 3, respectively). Both shRNAs targeting FOXO3A inhibited growth of KM-H2, U-HO1, HDLM2, and SUP-HD1 cell lines. L428 and L540 cell lines responded only to 1 of the 2 shRNAs, and L1236 cells were resistant to the antitumor effect of FOXO3A knockdown (Figure 6C). Neither of the cell lines was sensitive to at least 2 of the FOXO1-targeting shRNAs. Moreover, at least 2 of the shRNAs targeting FOXO1 stimulated proliferation of L428 and L1236 (supplemental Figure 3A). Knockdown efficiencies and the specificity of all shRNAs were confirmed with immunoblot (Figure 6D and supplemental Figure 3B, respectively).

**Figure 3 (continued)** (C) FOXO3A activation decreases the proportion of cells in the S phase. A total of  $1 \times 10^6$  cells were seeded in 10 mL of complete medium and treated with 4-OHT or with vehicle. After 24 hours, cells were harvested and cell cycle was analyzed by PI staining. Bars represent mean  $\pm$  SD of 3 independent experiments. Significance was calculated using a 2-sided t test. \* $P < .05$ ; \*\* $P < .01$ ; \*\*\* $P < .001$ ; \*\*\*\* $P < .0001$ .

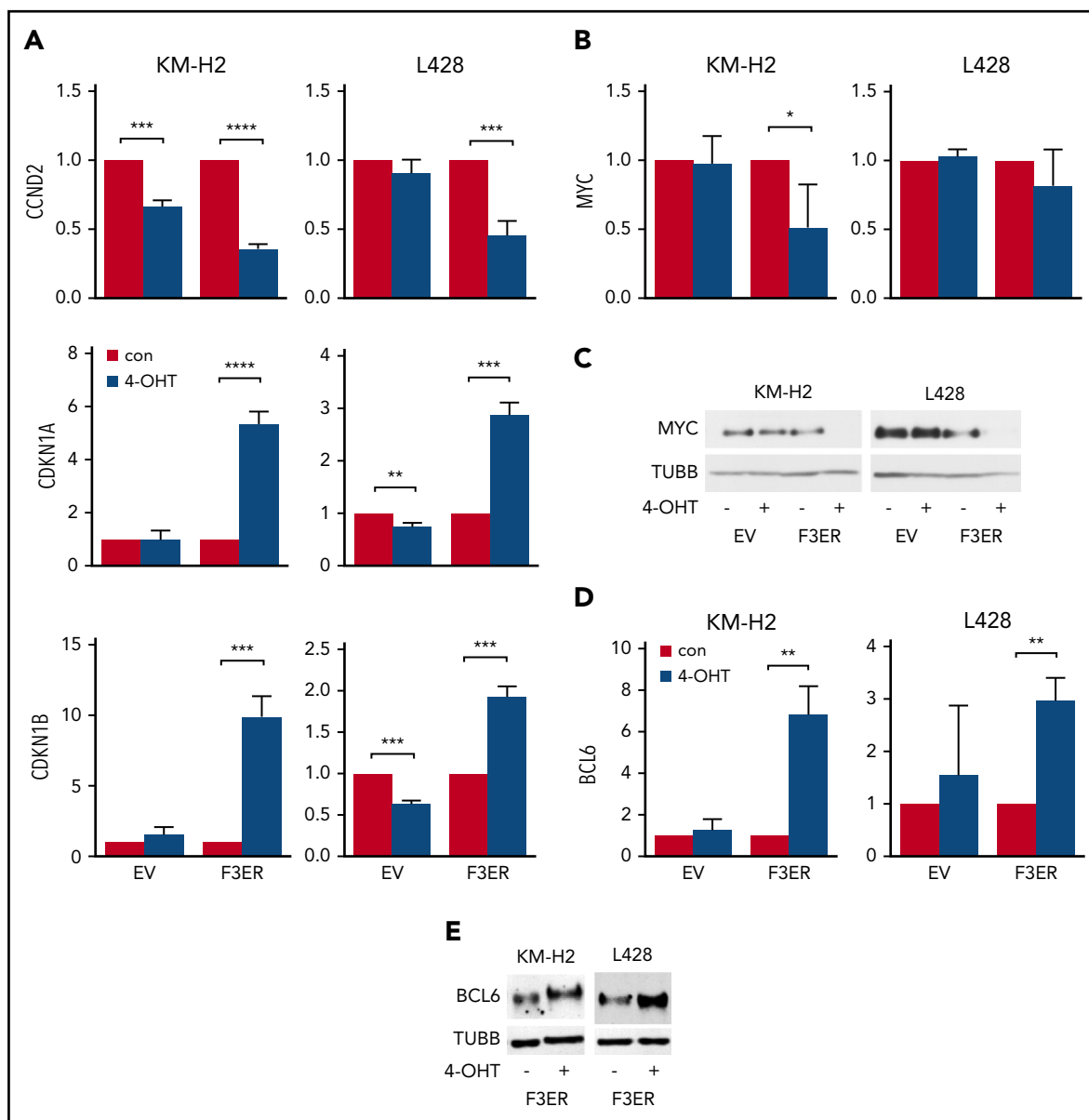


**Figure 4. FOXO3A-induced growth arrest correlates with upregulation of antiproliferative FOXO target genes.** cHL cell lines stably expressing FOXO3(A3)ER (F3ER) or EV were treated with 200 nM 4-OHT or vehicle. After 24 hours, cells were harvested and the expression of FOXO target genes was measured by RT-qPCR or immunoblot, respectively. (A) FOXO3A modulates expression of genes involved in proliferation. (B-C) FOXO3A downregulates MYC at mRNA (B) and protein level (C). (D-E) BCL6 is induced by FOXO3A both at mRNA (D) and protein (E) level. All RT-qPCR data are shown as relative expressions and mean  $\pm$  SD of 3 independent experiments. *RPL13A* was used as a reference gene for RT-qPCR and TUBB for immunoblot, respectively. The most representative immunoblots of 3 independent experiments are shown. Significance was calculated using a 2-sided t test. \* $P < .05$ ; \*\* $P < .01$ ; \*\*\* $P < .001$ ; \*\*\*\* $P < .0001$ .

Thus, maintenance of FOXO3A activity contributes to the oncogenic program of cHL independent of their origin.

## Discussion

We revealed an inverse dynamic of FOXO1 and FOXO3A expression during the process of GC maturation into memory cells and PCs. cHL, which is suggested to have an aborted PC-differentiation phenotype, expressed levels of FOXO3A intermediate between GC B cells and PCs. Overexpression of FOXO3A in cHL-inhibited cell proliferation but did not induce prominent cell death. We identified chromosomal deletions,<sup>4</sup> *MIR155* expression, and ERK activation as additional mechanisms

limiting FOXO3A expression in cHL. Finally, we show that tight regulation of FOXO3A contributes to the maintenance of cHL.

Although FOXO transcription factors are ubiquitously expressed, the expression levels of individual members differ.<sup>19,30,38,39</sup> In this study, we describe an increasing FOXO3A-to-FOXO1 ratio during the process of B-cell development. There are several lines of evidence that hint at a role of FOXO3A in PC differentiation. FOXO3 is among the genes that were most strongly upregulated in B cells committed to PC differentiation.<sup>25,26</sup> In human multiple myeloma, a PC malignancy, FOXO3A transcription is driven by a superenhancer similar to the regulation of other critical genes of the PC program including *IGH*, *IGL*, *IGK*, *IGJ*, and *PRDM1*.<sup>55</sup>

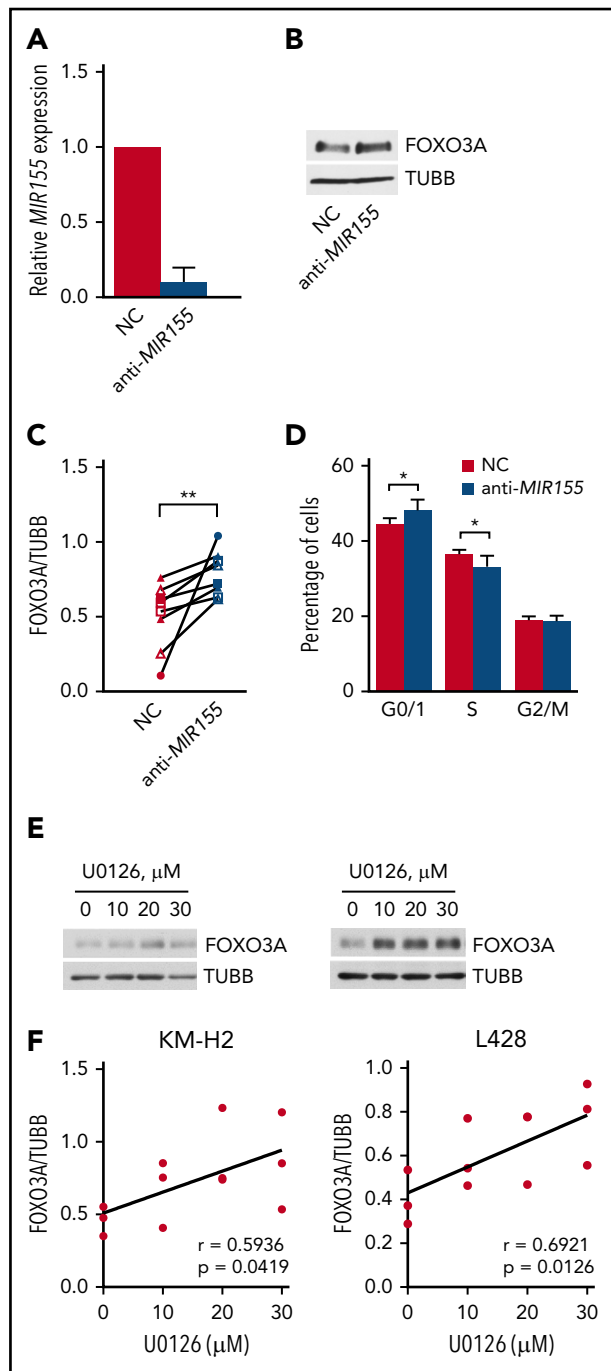


**Figure 5. *MIR155* and ERK regulate FOXO3A expression in cHL.** (A-C) *MIR155* contributes to FOXO3A repression. *MIR155* was inhibited in the cell line L428 with a miScript miRNA inhibitor (anti-*MIR155*; Qiagen) compared with a negative control (NC). (A) The efficiency of *MIR155* inhibition was confirmed by RT-qPCR 24 hours after transfection. (B) After 72 hours, the effect of *MIR155* inhibition on FOXO3A protein levels was evaluated using immunoblot analysis. A representative of 8 experiments is shown. (C) Immunoblots from panel B were quantified using ImageJ 64 and significance was calculated by a 2-sided t test using GraphPad Prism software. (D) *MIR155* inhibition leads to cell-cycle arrest in L428 72 hours after transfection. Data of 3 independent experiments are shown as mean  $\pm$  SD. Significances were calculated by a 2-sided t test using GraphPad Prism software.  $**P < .01$ . (E-F) ERK mitigates FOXO3A expression. KM-H2 and L428 were treated with the ERK inhibitor U0126 or vehicle. (E) After 24 hours, cells were lysed and total FOXO3A levels were assessed with immunoblot. A representative of 3 experiments is shown. (F) Dose-dependent activation of FOXO3A by the ERK inhibitor U0126. ImageJ 64 was used to quantify immunoblots obtained in panel E. Pearson correlation coefficient “r” and the P value were calculated using GraphPad Prism 6.

Recently, we reported the ability of FOXO1 to activate *PRDM1 $\alpha$*  transcription in cHL cell lines.<sup>15</sup> Interestingly, *PRDM1* is strongly induced by FOXO3A and by CTNNB1/ $\beta$ -catenin in human colon carcinoma cell lines.<sup>56</sup> Of note, these data contradict the observation of increased serum levels of immunoglobulin subtypes after genetic ablation of Foxo3 in mice.<sup>22</sup> This discrepancy might be explained by compensatory mechanisms of other FOXO family members for the deletion of FOXO3A, or by interspecies differences.

It is worth mentioning that the high FOXO3A-to-FOXO1 ratio in cHL, which was similar to the expression levels found in PCs, urged us to reconsider the main mechanism of FOXO1 repression in cHL. It is conceivable that FOXO1 repression primarily reflects the origin of HRS cells from a B cell committed to PC differentiation, and that chromosomal aberrations and epigenetic processes might play an auxiliary role in FOXO1 inactivation in cHL.

We found that overexpression of FOXO3A inhibits growth of cHL cell lines. In general, FOXOs are considered to act as tumor suppressors in diverse tumor entities<sup>57-59</sup> including cHL, as we have shown earlier for FOXO1.<sup>19</sup> Frequent deletions of FOXO3A that correlate with decreased FOXO3A expression levels<sup>4</sup> also indicate a tumor-suppressor role of FOXO3A in cHL. Of note, we found that, in cHL, FOXO3A differs from FOXO1 in a way that FOXO3A induces growth arrest but not apoptosis as FOXO1 does.<sup>19</sup> Interestingly, overexpression of wild-type FOXO3A also does not induce cell death in purified B cells from Balb/c mice but caused a delay in cell-cycle progression.<sup>60</sup> Our results are in line with a previously suggested role of FOXO3A as a stemness factor in cHL.<sup>61</sup> In clinical samples, expression of FOXO3A was reported to be limited to mononuclear Hodgkin cells, whereas multinucleated, more differentiated Reed-Stemberg cells were negative.<sup>61</sup> Moreover, the FOXO3A-expressing population in cHL cell lines demonstrated a higher ability to form colonies in methyl cellulose and to induce tumor formation in NOD/SCID mice.<sup>61</sup> Another possible explanation of the low apoptogenic activity of FOXO3A in cHL could be high expression of the SIRT1 deacetylase in HRS cells and in cHL cell lines.<sup>62</sup> Deacetylation of FOXO3A by SIRT1 is known to decrease its apoptogenic activity.<sup>63</sup>

In the present study, we identified the oncogenic miRNA *MIR155* as a negative regulator of FOXO3A in cHL. Down-regulation of FOXO3A by *MIR155* is already known to contribute to invasion and proliferation of glioma cells<sup>53</sup> as well as to resistance of lung cancer to gefitinib.<sup>64</sup> However, we did not observe a correlation between *MIR155* and FOXO3A expression (data not shown), indicating that FOXO3A is not exclusively regulated by *MIR155* in cHL. We also found that ERK activation is an additional factor controlling FOXO3A expression in cHL. Constitutive activation of ERK is well known to occur in cHL<sup>65</sup> and we also observed ERK phosphorylation in KM-H2 and L428 earlier.<sup>19</sup> Similar to our results for FOXO1,<sup>19</sup> we could demonstrate upregulation of FOXO3A by ERK inhibition.

In addition, we found that hyperactivation of the FOXO-inactivating kinase AKT as well as FOXO3A knockdown repressed growth in most cHL cell lines. Interestingly, FOXO1 demonstrates a similar bimodal effect on proliferation of endothelial cells.<sup>66</sup> The necessity of tight regulation of AKT activation was already demonstrated in pre-B-cell acute lymphoblastic leukemia. Although pre-B-cell



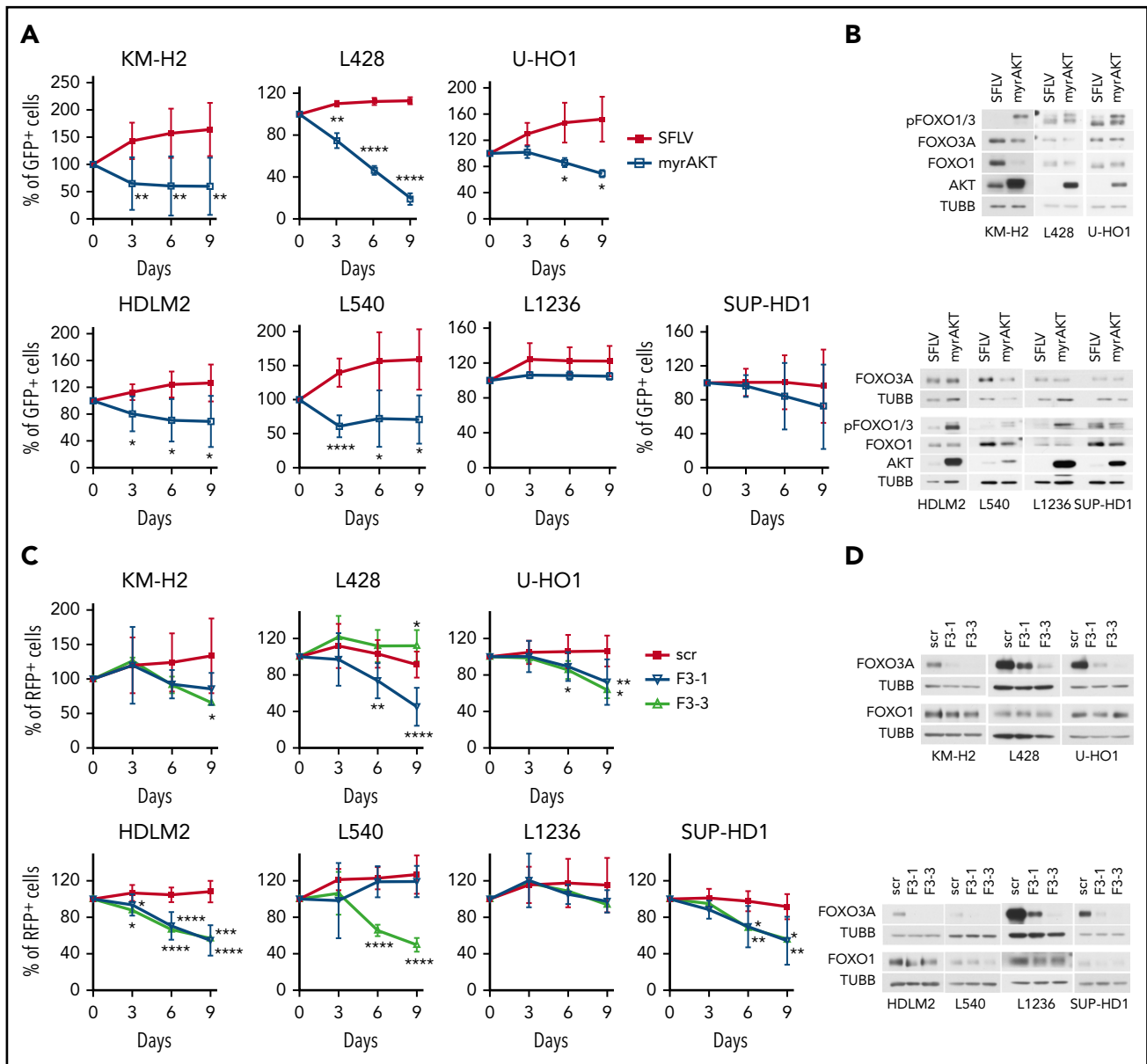


**Figure 6. FOXO3A knockdown shows an antitumor effect in cHL cell lines.** cHL cell lines were transduced with indicated lentiviral plasmids as described in "Materials and methods." The dynamic of transduced cells was followed starting from the fifth day after transduction (day 0) and the percentage of fluorescent cells on day 0 was set as 100%. Fluorescence was measured every third day using flow cytometry. (A) Constitutive AKT activation (myrAKT) decreased the percentage of green fluorescent protein-positive (GFP<sup>+</sup>) cells in cHL cell lines except for L1236 and SUP-HD1. (B) Immunoblot was performed after sorting of GFP<sup>+</sup> cells to confirm overexpression of myrAKT and FOXO inactivation. (C) Effect of FOXO3A shRNAs on the red fluorescent protein-positive (RFP<sup>+</sup>) population in cHL. (D) Protein of RFP<sup>+</sup> cells was isolated after selection with puromycin for 2 days (4  $\mu$ g/mL). shRNA efficiencies and specificities were confirmed with immunoblot. TUBB served as loading control for immunoblot analysis. All experiments were performed for at least 3 times and kinetics are shown as mean  $\pm$  SD. Significance was calculated compared with the scrambled control using a 2-sided *t* test. \**P* < .05; \*\**P* < .01; \*\*\**P* < .001; \*\*\*\**P* < .0001. F3-1, FOXO3A shRNA-1; F3-3, FOXO3A shRNA-3; scr, scrambled control.

acute lymphoblastic leukemias depend on oncogenic AKT activation, knockdown of the negative phosphatidylinositol 3-kinase-AKT regulator phosphatase and tensin homolog or overexpression of myrAKT is toxic for them.<sup>67</sup> In our experiments, myrAKT overexpression was not (L1236) or only merely toxic (SUP-HD1) in cell lines in which AKT is activated.<sup>19</sup> Of note, even cells addicted to oncogenic AKT activation still show nuclear expression of FOXOs.<sup>68,69</sup> Interestingly, toxicity of AKT overactivation is lineage-specific and was attributed to B cells but not to the myeloid lineage.<sup>67</sup> cHL not only has lost most of the B-cell program, but, in addition, often demonstrates features of myeloid

and T-cell lineages.<sup>70</sup> Therefore, resistance of L1236 and SUP-HD1 to myrAKT overexpression might be mediated not only by the inability to further inactivate FOXO3A (SUP-HD1), but also by the consequence of loss of B-cell program and/or transdifferentiation (L1236). Although other mechanisms might be involved, FOXO3A knockdown in general reproduced the antitumor effect of AKT hyperactivation. In particular, L1236, the cell line most resistant to myrAKT overexpression, was also resistant to FOXO3A knockdown, whereas other cell lines appeared to be sensitive to different extents. Given the role of FOXO3A as a stemness factor in cHL, this finding is not completely unexpected.<sup>61</sup> FOXO3A is

known to act as an oncogene in acute myeloid leukemia and is involved in chemoresistance. In particular, FOXO3A knockdown resulted in myeloid differentiation and cell death in acute myeloid leukemia.<sup>71,72</sup> In chronic myeloid leukemia, *Foxo3a* was found to be responsible for the resistance of leukemia-initiating cells to the BCR-ABL1 inhibitor imatinib.<sup>73</sup>

Further investigation of molecular mechanisms underlying the role of FOXO3A on cHL progression might provide a rationale for FOXO3A modulation in cHL treatment.

Taken together, our data indicate that intermediate FOXO3A expression levels between GC B cells and PCs reflect the abortive PC differentiation status of cHL and that the specific balance of FOXO transcription factors might contribute to the cHL oncogenic program. At the same time, excessive FOXO3A activation seems to negatively influence proliferation of HRS cells. FOXO3A levels thus need to be restrained, among others, by *MIR155* and by constitutive activation of ERK to maintain cHL integrity.

## Acknowledgments

The authors thank Anita Kick for excellent technical assistance. The authors thank the Core Facility FACS (Medical Faculty, University of Ulm) for sorting and Michaela Buck as well as Elena Kelsch (Institute of Pathology, University of Ulm) for short-tandem-repeat analysis.

F.G. was supported by the International Graduate School in Molecular Medicine, Ulm. This work was partially supported by Deutsche Krebshilfe eV (grant 110564) (T.W., A.U.).

## Authorship

Contribution: C.D.O., L.X., H.G., F.H., S.M.P., M.J.V., F.G., F.C.C., C.S., and A.U. performed research and analyzed data; and C.D.O., T.W., and A.U. designed research and wrote the manuscript.

Conflict-of-interest disclosure: The authors declare no competing financial interests.

Correspondence: Thomas Wirth, Institute of Physiological Chemistry, University of Ulm, Albert-Einstein-Allee 11, 89081 Ulm, Germany; e-mail: thomas.wirth@uni-ulm.de; and Alexey Ushmorov, Institute of Physiological Chemistry, University of Ulm, Albert-Einstein-Allee 11, 89081 Ulm, Germany; e-mail: alexey.ushmorov@uni-ulm.de.

## Footnotes

Submitted 10 July 2017; accepted 12 February 2018. Prepublished online as *Blood* First Edition paper, 13 February 2018; DOI 10.1182/blood-2017-07-795278.

The online version of this article contains a data supplement.

The publication costs of this article were defrayed in part by page charge payment. Therefore, and solely to indicate this fact, this article is hereby marked "advertisement" in accordance with 18 USC section 1734.

## REFERENCES

- Tiacci E, Döring C, Brune V, et al. Analyzing primary Hodgkin and Reed-Sternberg cells to capture the molecular and cellular pathogenesis of classical Hodgkin lymphoma. *Blood*. 2012;120(23):4609-4620.
- Müschen M, Rajewsky K, Bräuninger A, et al. Rare occurrence of classical Hodgkin's disease as a T cell lymphoma. *J Exp Med*. 2000;191(2):387-394.
- Küppers R, Engert A, Hansmann ML. Hodgkin lymphoma. *J Clin Invest*. 2012;122(10):3439-3447.
- Steidl C, Diepstra A, Lee T, et al. Gene expression profiling of microdissected Hodgkin Reed-Sternberg cells correlates with treatment outcome in classical Hodgkin lymphoma. *Blood*. 2012;120(17):3530-3540.
- Jundt F, Anagnostopoulos I, Förster R, Mathas S, Stein H, Dörken B. Activated Notch1 signaling promotes tumor cell proliferation and survival in Hodgkin and anaplastic large cell lymphoma. *Blood*. 2002;99(9):3398-3403.
- Re D, Müschen M, Ahmadi T, et al. Oct-2 and Bob-1 deficiency in Hodgkin and Reed Sternberg cells. *Cancer Res*. 2001;61(5):2080-2084.
- Mathas S, Janz M, Hummel F, et al. Intrinsic inhibition of transcription factor E2A by HLH proteins ABF-1 and Id2 mediates reprogramming of neoplastic B cells in Hodgkin lymphoma. *Nat Immunol*. 2006;7(2):207-215.
- Schmid C, Pan L, Diss T, Isaacson PG. Expression of B-cell antigens by Hodgkin's and Reed-Sternberg cells. *Am J Pathol*. 1991;139(4):701-707.
- Tzankov A, Zimpfer A, Pehrs AC, et al. Expression of B-cell markers in classical Hodgkin lymphoma: a tissue microarray analysis of 330 cases. *Mod Pathol*. 2003;16(11):1141-1147.
- Carbone A, Ghoghini A, Gaidano G, et al. Expression status of BCL-6 and syndecan-1 identifies distinct histogenetic subtypes of Hodgkin's disease. *Blood*. 1998;92(7):2220-2228.
- Foss HD, Reusch R, Demel G, et al. Frequent expression of the B-cell-specific activator protein in Reed-Sternberg cells of classical Hodgkin's disease provides further evidence for its B-cell origin. *Blood*. 1999;94(9):3108-3113.
- Carbone A, Ghoghini A, Aldinucci D, Gattei V, Dalla-Favera R, Gaidano G. Expression pattern of MUM1/IRF4 in the spectrum of pathology of Hodgkin's disease. *Br J Haematol*. 2002;117(2):366-372.
- Buettner M, Greiner A, Avramidou A, Jäck HM, Niedobitek G. Evidence of abortive plasma cell differentiation in Hodgkin and Reed-Sternberg cells of classical Hodgkin lymphoma. *Hematol Oncol*. 2005;23(3-4):127-132.
- Seitz V, Thomas PE, Zimmermann K, et al. Classical Hodgkin's lymphoma shows epigenetic features of abortive plasma cell differentiation. *Haematologica*. 2011;96(6):863-870.
- Vogel MJ, Xie L, Guan H, et al. FOXO1 repression contributes to block of plasma cell differentiation in classical Hodgkin lymphoma. *Blood*. 2014;124(20):3118-3129.
- Mandelbaum J, Bhagat G, Tang H, et al. BLIMP1 is a tumor suppressor gene frequently disrupted in activated B cell-like diffuse large B cell lymphoma. *Cancer Cell*. 2010;18(6):568-579.
- Küppers R, Klein U, Schwering I, et al. Identification of Hodgkin and Reed-Sternberg cell-specific genes by gene expression profiling. *J Clin Invest*. 2003;111(4):529-537.
- Tam W, Gomez M, Chadburn A, Lee JW, Chan WC, Knowles DM. Mutational analysis of PRDM1 indicates a tumor-suppressor role in diffuse large B-cell lymphomas. *Blood*. 2006;107(10):4090-4100.
- Xie L, Ushmorov A, Leithäuser F, et al. FOXO1 is a tumor suppressor in classical Hodgkin lymphoma. *Blood*. 2012;119(15):3503-3511.
- Coffer PJ, Burgering BM. Forkhead-box transcription factors and their role in the immune system. *Nat Rev Immunol*. 2004;4(11):889-899.
- Eijkelenboom A, Burgering BM. FOXOs: signalling integrators for homeostasis maintenance. *Nat Rev Mol Cell Biol*. 2013;14(2):83-97.
- Hinman RM, Nichols WA, Diaz TM, Gallardo TD, Castrillon DH, Satterthwaite AB. Foxo3<sup>-/-</sup> mice demonstrate reduced numbers of pre-B and recirculating B cells but normal splenic B cell sub-population distribution. *Int Immunol*. 2009;21(7):831-842.
- Dengler HS, Baracho GV, Omori SA, et al. Distinct functions for the transcription factor Foxo1 at various stages of B cell differentiation. *Nat Immunol*. 2008;9(12):1388-1398.
- Su YW, Hao Z, Hirao A, et al. 14-3-3sigma regulates B-cell homeostasis through

- stabilization of FOXO1 [published corrections appear in *Proc Natl Acad Sci USA*. 2011; 108(16):6689 and *Proc Natl Acad Sci USA*. 2013;110(39):15849]. *Proc Natl Acad Sci USA*. 2011;108(4):1555-1560.
25. Cocco M, Stephenson S, Care MA, et al. In vitro generation of long-lived human plasma cells. *J Immunol*. 2012;189(12):5773-5785.
26. Tooze RM. A replicative self-renewal model for long-lived plasma cells: questioning irreversible cell cycle exit. *Front Immunol*. 2013;4:460.
27. Ikeda J, Tian T, Wang Y, et al. Expression of FoxO3a in clinical cases of malignant lymphoma. *Pathol Res Pract*. 2013;209(11):716-720.
28. Ikeda JI, Wada N, Nojima S, et al. ID1 upregulation and FoxO3a downregulation by Epstein-Barr virus-encoded LMP1 in Hodgkin's lymphoma. *Mol Clin Oncol*. 2016;5(5):562-566.
29. Guan H, Xie L, Leithäuser F, et al. KLF4 is a tumor suppressor in B-cell non-Hodgkin lymphoma and in classic Hodgkin lymphoma. *Blood*. 2010;116(9):1469-1478.
30. Bakker WJ, van Dijk TB, Parren-van Amelsvoort M, et al. Differential regulation of Foxo3a target genes in erythropoiesis. *Mol Cell Biol*. 2007;27(10):3839-3854.
31. Ramaswamy S, Nakamura N, Vazquez F, et al. Regulation of G1 progression by the PTEN tumor suppressor protein is linked to inhibition of the phosphatidylinositol 3-kinase/Akt pathway. *Proc Natl Acad Sci USA*. 1999;96(5):2110-2115.
32. Hruz T, Laule O, Szabo G, et al. Genevestigator v3: a reference expression database for the meta-analysis of transcriptomes. *Adv Bioinformatics*. 2008;2008:420747.
33. Hruz T, Wyss M, Docquier M, et al. RefGenes: identification of reliable and condition specific reference genes for RT-qPCR data normalization. *BMC Genomics*. 2011;12(1):156.
34. Li Q, Birkbak NJ, Györfy B, Szallasi Z, Eklund AC. Jetset: selecting the optimal microarray probe set to represent a gene. *BMC Bioinformatics*. 2011;12(1):474.
35. Xie L, Ritz O, Leithäuser F, et al. FOXO1 downregulation contributes to the oncogenic program of primary mediastinal B-cell lymphoma. *Oncotarget*. 2014;5(14):5392-5402.
36. Turrel-Davin F, Tournadre A, Pachot A, et al. FoxO3a involved in neutrophil and T cell survival is overexpressed in rheumatoid blood and synovial tissue. *Ann Rheum Dis*. 2010;69(4):755-760.
37. Jourdan M, Caraux A, De Vos J, et al. An in vitro model of differentiation of memory B cells into plasmablasts and plasma cells including detailed phenotypic and molecular characterization. *Blood*. 2009;114(25):5173-5181.
38. Dominguez-Sola D, Kung J, Holmes AB, et al. The FOXO1 transcription factor instructs the Germinal Center Dark Zone Program. *Immunity*. 2015;43(6):1064-1074.
39. Sander S, Chu VT, Yasuda T, et al. PI3 kinase and FOXO1 transcription factor activity differentially control B cells in the germinal center light and dark zones. *Immunity*. 2015;43(6):1075-1086.
40. Kamesaki H, Fukuhara S, Tatsumi E, et al. Cytochemical, immunologic, chromosomal, and molecular genetic analysis of a novel cell line derived from Hodgkin's disease. *Blood*. 1986;68(1):285-292.
41. Drexler HG. Recent results on the biology of Hodgkin and Reed-Sternberg cells. II. Continuous cell lines. *Leuk Lymphoma*. 1993;9(1-2):1-25.
42. Schaadt M, Diehl V, Stein H, Fonatsch C, Kirchner HH. Two neoplastic cell lines with unique features derived from Hodgkin's disease. *Int J Cancer*. 1980;26(6):723-731.
43. Mader A, Bruderlein S, Wegener S, et al. U-HO1, a new cell line derived from a primary refractory classical Hodgkin lymphoma. *Cytogenet Genome Res*. 2007;119(3-4):204-210.
44. Kanzler H, Hansmann ML, Kapp U, et al. Molecular single cell analysis demonstrates the derivation of a peripheral blood-derived cell line (L1236) from the Hodgkin/Reed-Sternberg cells of a Hodgkin's lymphoma patient. *Blood*. 1996;87(8):3429-3436.
45. Naumovski L, Utz PJ, Bergstrom SK, et al. SUP-HD1: a new Hodgkin's disease-derived cell line with lymphoid features produces interferon-gamma. *Blood*. 1989;74(8):2733-2742.
46. Diehl V, Kirchner HH, Schaadt M, et al. Hodgkin's disease: establishment and characterization of four in vitro cell lines. *J Cancer Res Clin Oncol*. 1981;101(1):111-124.
47. Thelander EF, Ichimura K, Corcoran M, et al. Characterization of 6q deletions in mature B cell lymphomas and childhood acute lymphoblastic leukemia. *Leuk Lymphoma*. 2008;49(3):477-487.
48. van Boxtel R, Gomez-Puerto C, Mokry M, et al. FOXP1 acts through a negative feedback loop to suppress FOXO-induced apoptosis. *Cell Death Differ*. 2013;20(9):1219-1229.
49. Oestreich KJ, Mohn SE, Weinmann AS. Molecular mechanisms that control the expression and activity of Bcl-6 in TH1 cells to regulate flexibility with a TFH-like gene profile. *Nat Immunol*. 2012;13(4):405-411.
50. Fernández de Mattos S, Essafi A, Soeiro I, et al. FoxO3a and BCR-ABL regulate cyclin D2 transcription through a STAT5/BCL6-dependent mechanism. *Mol Cell Biol*. 2004;24(22):10058-10071.
51. Ferber EC, Peck B, Delpuech O, Bell GP, East P, Schulze A. FOXO3a regulates reactive oxygen metabolism by inhibiting mitochondrial gene expression. *Cell Death Differ*. 2012;19(6):968-979.
52. Gan B, Lim C, Chu G, et al. FoxOs enforce a progression checkpoint to constrain mTORC1-activated renal tumorigenesis. *Cancer Cell*. 2010;18(5):472-484.
53. Ling N, Gu J, Lei Z, et al. microRNA-155 regulates cell proliferation and invasion by targeting FOXO3a in glioma. *Oncol Rep*. 2013;30(5):2111-2118.
54. Kluiver J, Poppema S, de Jong D, et al. BIC and miR-155 are highly expressed in Hodgkin, primary mediastinal and diffuse large B cell lymphomas. *J Pathol*. 2005;207(2):243-249.
55. Affer M, Chesi M, Chen WG, et al. Promiscuous MYC locus rearrangements hijack enhancers but mostly super-enhancers to dysregulate MYC expression in multiple myeloma. *Leukemia*. 2014;28(8):1725-1735.
56. Tenbaum SP, Ordóñez-Morán P, Puig I, et al.  $\beta$ -catenin confers resistance to PI3K and AKT inhibitors and subverts FOXO3a to promote metastasis in colon cancer. *Nat Med*. 2012;18(6):892-901.
57. Obrador-Hevia A, Serra-Sitjar M, Rodríguez J, Villalonga P, Fernández de Mattos S. The tumour suppressor FOXO3 is a key regulator of mantle cell lymphoma proliferation and survival. *Br J Haematol*. 2012;156(3):334-345.
58. Paik JH, Kollipara R, Chu G, et al. FoxOs are lineage-restricted redundant tumor suppressors and regulate endothelial cell homeostasis. *Cell*. 2007;128(2):309-323.
59. Sunter A, Fernández de Mattos S, Stahl M, et al. FoxO3a transcriptional regulation of Bim controls apoptosis in paclitaxel-treated breast cancer cell lines. *J Biol Chem*. 2003;278(50):49795-49805.
60. Yusuf I, Zhu X, Kharas MG, Chen J, Fruman DA. Optimal B-cell proliferation requires phosphoinositide 3-kinase-dependent inactivation of FOXO transcription factors. *Blood*. 2004;104(3):784-787.
61. Ikeda J, Mamat S, Tian T, et al. Tumorigenic potential of mononucleated small cells of Hodgkin lymphoma cell lines. *Am J Pathol*. 2010;177(6):3081-3088.
62. Frazzi R, Valli R, Tamagnini I, Casali B, Latruffe N, Merli F. Resveratrol-mediated apoptosis of Hodgkin lymphoma cells involves SIRT1 inhibition and FOXO3a hyperacetylation. *Int J Cancer*. 2013;132(5):1013-1021.
63. Motta MC, Divecha N, Lemieux M, et al. Mammalian SIRT1 represses forkhead transcription factors. *Cell*. 2004;116(4):551-563.
64. Chiu CF, Chang YW, Kuo KT, et al. NF- $\kappa$ B-driven suppression of FOXO3a contributes to EGFR mutation-independent gefitinib resistance [published correction appears in *Proc Natl Acad Sci USA*. 2017;114(4):E654-E655]. *Proc Natl Acad Sci USA*. 2016;113(18):E2526-E2535.
65. Zheng B, Fiumara P, Li YV, et al. MEK/ERK pathway is aberrantly active in Hodgkin disease: a signaling pathway shared by CD30, CD40, and RANK that regulates cell proliferation and survival. *Blood*. 2003;102(3):1019-1027.
66. Dharaneeswaran H, Abid MR, Yuan L, et al. FOXO1-mediated activation of Akt plays a critical role in vascular homeostasis [published correction appears in *Circ Res*. 2014;115(4):e9.]. *Circ Res*. 2014;115(2):238-251.
67. Shojaee S, Chan LN, Buchner M, et al. PTEN opposes negative selection and enables oncogenic transformation of pre-B cells. *Nat Med*. 2016;22(4):379-387.
68. Ochodnicka-Mackovicova K, Bahjat M, Bloedjes TA, et al. NF- $\kappa$ B and AKT signaling prevent DNA damage in transformed pre-B cells by suppressing RAG1/2 expression and activity. *Blood*. 2015;126(11):1324-1335.

69. Köhrer S, Havranek O, Seyfried F, et al. Pre-BCR signaling in precursor B-cell acute lymphoblastic leukemia regulates PI3K/AKT, FOXO1 and MYC, and can be targeted by SYK inhibition. *Leukemia*. 2016;30(6):1246-1254.
70. Küppers R. The biology of Hodgkin's lymphoma. *Nat Rev Cancer*. 2009;9(1):15-27.
71. Santamaría CM, Chillón MC, García-Sanz R, et al. High FOXO3a expression is associated with a poorer prognosis in AML with normal cytogenetics. *Leuk Res*. 2009;33(12):1706-1709.
72. Sykes SM, Lane SW, Bullinger L, et al. AKT/FOXO signaling enforces reversible differentiation blockade in myeloid leukemias [published correction appears in *Cell*. 2011;147(1):247]. *Cell*. 2011;146(5):697-708.
73. Naka K, Hoshii T, Muraguchi T, et al. TGF-beta-FOXO signalling maintains leukaemia-initiating cells in chronic myeloid leukaemia. *Nature*. 2010;463(7281):676-680.